

# Intense $^{31-35}\text{Ar}$ beams produced with a nanostructured CaO target at ISOLDE



J.P. Ramos<sup>a,b</sup>, A. Gottberg<sup>a,c</sup>, T.M. Mendonça<sup>a,e</sup>, C. Seiffert<sup>a,f</sup>, A.M.R. Senos<sup>b</sup>, H.O.U. Fynbo<sup>d</sup>, O. Tengblad<sup>c</sup>, J.A. Briz<sup>c</sup>, M.V. Lund<sup>d</sup>, G.T. Koldste<sup>d</sup>, M. Carmona-Gallardo<sup>c</sup>, V. Pesudo<sup>c</sup>, T. Stora<sup>a,\*</sup>

<sup>a</sup> CERN, CH-1211 Genève 23, Switzerland

<sup>b</sup> Department of Materials and Ceramics Engineering, University of Aveiro, CICECO, 3810-193 Aveiro, Portugal

<sup>c</sup> Instituto de Estructura de la Materia, CSIC, Serrano 113 bis, E-28006 Madrid, Spain

<sup>d</sup> Department of Physics and Astronomy, University of Aarhus, DK-8000 Aarhus, Denmark

<sup>e</sup> IFIMUP-IN, Institute of Nanosciences and Nanotechnology, University of Porto, 4169-007 Porto, Portugal

<sup>f</sup> Technische Universität Darmstadt, Schlossgartenstraße 9, 64289 Darmstadt, Germany

## ARTICLE INFO

### Article history:

Received 29 August 2013

Received in revised form 6 December 2013

Available online 31 December 2013

### Keywords:

Calcium oxide

Argon beams

Radioactive ion beams

Exotic isotopes

CERN-ISOLDE

Nanomaterials

## ABSTRACT

At the ISOLDE facility at CERN, thick targets are bombarded with highly energetic pulsed protons to produce radioactive ion beams (RIBs). The isotopes produced in the bulk of the material have to diffuse out of the grain and effuse throughout the porosity of the material to a transfer line which is connected to an ionizer, from which the charged isotopes are extracted and delivered for physics experiments. Calcium oxide (CaO) powder targets have been used to produce mainly neutron deficient argon and carbon RIBs over the past decades. Such targets presented unstable yields, either decaying over time or low from the beginning of operation. These problems were suspected to come from the degradation of the target microstructure (sintering due to high temperature and/or high proton intensity). In this work, a CaO microstructural study in terms of sintering was conducted on a nanostructured CaO powder synthesized from the respective carbonate. Taking the results of this study, several changes were made at ISOLDE in terms of the CaO target production, handling and operation in order to produce and maintain the nanostructured CaO. The new target, the first nanostructured target to be operated at ISOLDE, showed improved yields of (exotic) Ar and more importantly a stable yield over the whole operation time, while operating with lower temperatures. This contradicts the ISOL paradigm of using the highest possible temperature regardless of the target's microstructure degradation.

© 2015 CERN for the benefit of the Authors. Published by Elsevier B.V. This is an open access article under the CC BY license (<http://creativecommons.org/licenses/by/4.0/>).

## 1. Introduction

ISOLDE (acronym for Isotope Separator OnLine DEvice) is a world-wide leading facility at CERN for the production of an extensive range of radioactive ion beams (RIBs) of various energies (up to 3.1 MeV per nucleon), for physics experiments in the areas of biophysics, astrophysics, nuclear, atomic and solid state physics. This facility is able to provide more than 1000 isotopes of 72 different elements with half-lives ( $T_{1/2}$ ) starting from a few milliseconds and with intensities from  $10^{-1}$  to  $10^{11}$  ions  $s^{-1}$  [1].

The ISOL (Isotope Separator OnLine) technique consists in bombarding thick targets (at ISOLDE, 2 cm diameter 20 cm long cylinder, from 5 to 200  $g\text{ cm}^{-2}$ ) with energetic protons (1.4 GeV) in order to promote the production of isotopes by nuclear spallation, fragmentation and fission reactions [1]. The produced isotopes then, diffuse out of the material bulk and effuse through the

material porosity and a transfer line to the ion source where they are ionized. They are then accelerated up to 60 keV and mass separated by a mass spectrometer using the Lorentzian principle, forming a secondary beam that is conducted to the physics experiments. The intensity ( $i$ ) of the secondary beam (or RIB) can be theoretically approached by the following expression [2]:

$$i = \theta \cdot \sigma \cdot \eta \cdot \varepsilon_{rel} \cdot \varepsilon_{is} \cdot \varepsilon_{sep} \cdot \varepsilon_{trans} \quad (1)$$

where  $\theta$  is the flux of the incident proton beam,  $\eta$  is the number of atoms of the target exposed to the proton beam per area unit and  $\sigma$  is the cross-section for the production of the desired isotope.  $\varepsilon_{rel}$  is the release efficiency from the unit,  $\varepsilon_{is}$  is the ion source efficiency and  $\varepsilon_{sep}$  and  $\varepsilon_{trans}$  are respectively, the mass separator transmission efficiency and the transport efficiency after the dipole magnet to the experimental setup.

$\varepsilon_{rel}$  is directly related with effusion and diffusion processes. Effusion is associated with the surface properties of the target and surrounding materials, such as adsorption enthalpy [3]. The effusion efficiency can, as a first approximation, be enhanced by

\* Corresponding author. Tel.: +41 22 487 08 08.

E-mail address: [thierry.stora@cern.ch](mailto:thierry.stora@cern.ch) (T. Stora).

having the target volume as small as possible and the highest possible temperatures. Diffusion times can be reduced by developing and controlling the target material microstructure, mainly in terms of grain size and porosity [4]. From the two, diffusion is limiting the release in most cases, especially for the case of very exotic isotopes where  $T_{1/2}$  is short and diffusion times are typically larger [5]. Diffusion is mainly dependent on the species, host material and temperature since this process is thermally activated following an Arrhenius expression [6]:

$$D = D_0 \cdot e^{-\frac{Q}{RT}} \quad (2)$$

where  $D$  is the diffusion coefficient,  $D_0$  is the temperature-independent pre-exponential factor,  $Q$  is the activation energy,  $R$  is the universal gas constant and  $T$  is the absolute temperature. The maximum temperature is mainly limited by target sintering. Sintering brings grain growth, coarsening and porosity reduction, which negatively impacts the release process, increasing the diffusion lengths and so the diffusion times. This is most severe in the case of very exotic isotopes with short half-lives. The upper limit for the temperature is also affected by stable beam contaminants, coming from the target material and the equilibrium vapor pressure which has to be compatible with the operation of the ion source ( $<10^{-1}$  Pa in the standard operation mode of the Versatile Arc Discharge Ion Source – VADIS) [7,8].

Micrometric oxide or carbide powders (or fibers) are used at ISOLDE as target materials [7]. However it was shown recently, that targets with nanometric (or submicrometric) grain sizes and high porosity (>30%) with a macrosized (>100 nm) narrow distribution, improved the release properties of alkali metals, alkaline earth metals and noble gases [9]. Moreover, a successful attempt was also made in the past, at the TRIUMF facility with zeolites as target material, operated below 500 °C to produce better yields of radioactive  $^{16}\text{N}$  (and  $^{16}\text{N}^{14}\text{N}$  and  $^{16}\text{N}^{16}\text{O}$ ) [10].

Calcium oxide (CaO) powder targets have been operated at ISOLDE since 1985 [11] and are used to provide intense neutron deficient argon, carbon (produced as  $^{x}\text{C}^{16}\text{O}^+$  or  $^{x}\text{C}^{16}\text{O}_2^+$ ), helium and neon beams at high temperatures (950–1420 °C) [12,13,7]. These targets outperform others to produce the same beams, due to the high production cross sections and fast release times, but often suffer a either rapidly decreasing yield over time or low yields from the beginning. This problem was suspected to be microstructure-related, specifically to degradation induced by sintering effects [12].

This target material was mostly used to produce beams of  $^{31}\text{Ar}$  ( $T_{1/2} = 15.1$  ms),  $^{32}\text{Ar}$  ( $T_{1/2} = 98$  ms) and for  $^{35}\text{Ar}$  ( $T_{1/2} = 1.78$  s), respectively for studies in the fields of astrophysics [14] and nuclear physics [15–19]. The problems found in the delivery of the required beams with acceptable intensities over time, could easily jeopardize the experiments, justifying the investigation and beam development of these targets. As the target material was identified to be the source of the problem, a material investigation in terms of synthesis, air reactivity and sintering was done in order to develop a highly porous nanostructured CaO powder and to avoid its degradation, during production, handling and operation at ISOLDE [20,21]. Improved and stable yields (on exotic isotopes) were obtained while operating a nanostructured CaO powder target at a lower temperature and a lower proton intensity than is normally used.

## 2. Experimental procedure

### 2.1. Calcium oxide – synthesis and sintering studies

The material studies were done at the Department of Materials and Ceramics Engineering at the University of Aveiro (DEMaC-UA)

and can be found in detail in [20,21]. A brief overview of the studies will be done here.

To obtain CaO nanometric powder, a micrometric  $\text{CaCO}_3$  powder ( $<5$   $\mu\text{m}$ , 99.5% pure – metal basis) from Alfa Aesar GmbH, Germany was decomposed in a vertical alumina tube furnace at 800 °C under vacuum ( $10^{-2}$  Pa) for 2 h. Using nitrogen adsorption at liquid nitrogen temperatures, the specific surface area – SSA – (Brunauer, Emmett, Teller model – BET [22]) and mesopore (2–50 nm) size and volume (Barrett, Joyner, Halenda model – BJH [23]) were measured. The crystallite size was determined using X-ray diffraction (XRD) peak broadening with the Scherrer equation [24]. As shown in Table 1, the obtained material showed a high SSA, nanometric crystallite size (32 nm) and high porosity (44%) with 12 nm of average pore size. The final powder is also highly reactive in air to  $\text{H}_2\text{O}$  and  $\text{CO}_2$ , forming respectively  $\text{Ca}(\text{OH})_2$  and  $\text{CaCO}_3$ .

Transmission electron microscopy (TEM) was performed in order to confirm the characteristics shown in Table 1. As can be seen in Fig. 1, the sample shows (sub)micrometer particles which are porous agglomerates of nanometric grains. The obtained powder matches all the good characteristics referred before, for an ISOLDE target material except the pore size, which is a characteristic consequence of the used synthesis process.

From the obtained powder, 60% porous cylindrical compacts of 10 mm diameter by 2–3 mm thickness were pressed and sintered in a high vacuum furnace ( $<10^{-3}$  Pa), from 900 to 1250 °C with holding times from 3 min to 10 h. The SSA is a very sensitive parameter to evaluate the initial sintering of fine powders. SSA variation results, at different sintering temperatures for 10 h are presented in Fig. 2. It can be seen that net sintering effects are observed above 1000 °C with the reduction of SSA.

In order to keep the CaO nanostructure, the material must not be exposed to temperatures higher than 1000 °C, especially for the production of exotic isotopes ( $^{31}\text{Ar}$  and  $^{32}\text{Ar}$ ) where short diffusion lengths (which should provide faster release times) are crucial. Nonetheless sintering by proton irradiation [4] must also be

**Table 1**

Characteristics of CaO powder, obtained from decomposition of  $\text{CaCO}_3$  at 800 °C for 2 h, in vacuum, at the University of Aveiro.

Characteristics	Value	Technique
SSA	$58 \pm 4 \text{ m}^2 \text{ g}^{-1}$	BET
Porosity	$0.23 \text{ cm}^3 \text{ g}^{-1}$ (44%)	BJH
Average pore size	12 nm	BJH
Crystallite size	$32 \pm 1 \text{ nm}$	XRD

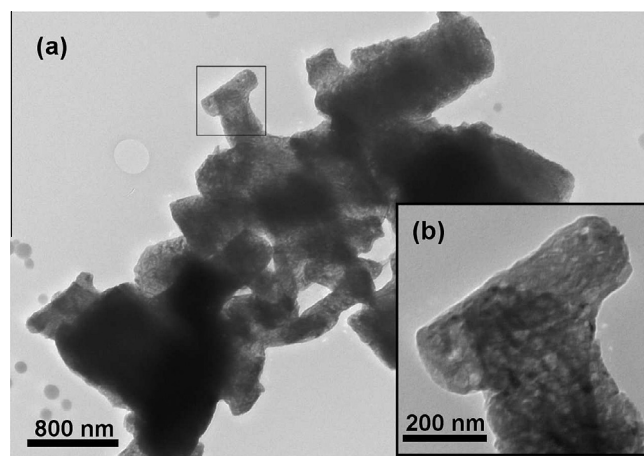


**Fig. 1.** CaO microstructure investigated by TEM at magnification 31500 $\times$  (a) and 229000 $\times$  (b).

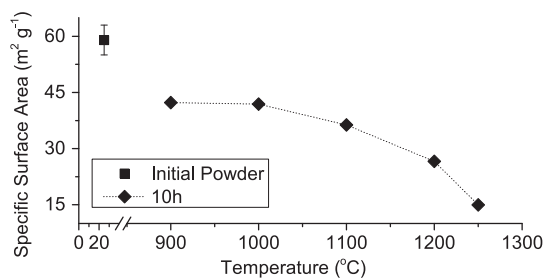


Fig. 2. SSA evolution with temperature for 10 h of holding time. The isolated point corresponds to the initial powder.

Table 2

Characteristics of CaO powder target, obtained from decomposition of CaCO<sub>3</sub> at 800 °C for 48 h, in vacuum, at CERN.

Characteristics	Value
SSA	37 m <sup>2</sup> g <sup>-1</sup>
Porosity	0.26 cm <sup>3</sup> g <sup>-1</sup> (47%)
Average pore size	23 nm
Crystallite size	37 nm
Target thickness	7.3 g cm <sup>-2</sup>
Target density	0.38 g cm <sup>-3</sup>

taken into account in such way that the target operation temperature and proton intensity must be carefully chosen in order to avoid the CaO nanostructure degradation and maintain acceptable release of the isotopes of interest.

## 2.2. Target production

Following the material studies done at the University of Aveiro a target unit was produced with the newly developed material, through a new procedure, for online studies. The CaCO<sub>3</sub> used to produce the old CaO targets was changed to the one used in the material studies in Section 2.1. The CaCO<sub>3</sub> was loaded into a rhenium boat, and heated up in vacuum until 800 °C, at a heating rate of 10 °C min<sup>-1</sup>, for 48 h. To avoid hydration and carbonation of the newly synthesized nanometric CaO, the production procedure was optimized: in the old procedure the rhenium boat would be refilled and reheated in order to account for the mass loss due to the decomposition reaction, which was not done in the optimized procedure. Furthermore, the boat was transferred inside a glove box, in a controlled atmosphere of Argon, to the target unit. Samples from the produced target material were taken for material characterization (Table 2). The target unit, labeled #469, had a water cooled transfer line with a forced electron beam induced arc discharge ion source, a VADIS which very efficiently ionizes

Table 3

Changes in the production, handling and operation conditions of the new CaO target (#469).

		Before [12] <sup>a</sup>	New procedure (#469)
Production	Raw material	≈14 μm 99% pure CaCO <sub>3</sub>	>5 μm 99.5% pure CaCO <sub>3</sub>
	Max. temperature	1200 °C	800 °C
	Heating/cooling	Not defined	10 °C min <sup>-1</sup>
	Holding time	Not defined	≈48 h
	Base pressure	10 <sup>-3</sup> Pa	10 <sup>-3</sup> Pa
Handling conditions	No cares taken against hydration and carbonation of CaO		Gloves box with an argon atmosphere for material handling
Operation	Temperature	950–1420 °C	up to 800 °C
	Temp. control	None. Calibration before with Pyrometer	Thermocouples in the side and center of the target
	Heating/cooling	Not defined	10 °C min <sup>-1</sup>
	Proton intensity	3 × 10 <sup>13</sup> ppp	8 × 10 <sup>12</sup> ppp

<sup>a</sup> CaO targets until 2009 (#419).

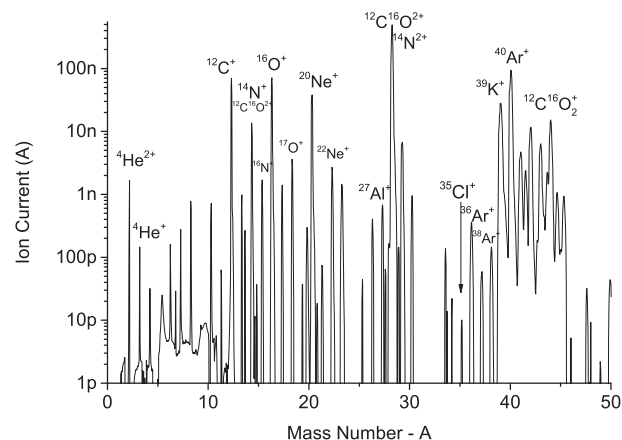


Fig. 3. Offline mass scan of the target CaO#469 until A = 50 with <sup>35</sup>Cl and other peaks identified.

noble gases [25]. Along the target container (at the center and side) two type K thermocouples were placed for additional temperature control. The changes in the production, handling and operation of this new unit are summarized in Table 3.

The analysed sample from the target presented similar characteristics (Table 2) to those of the CaO from the studies in University of Aveiro, summarized in Table 1, even after 48 h at 800 °C. The SSA result, is consistent with the tendency towards low temperature values in Fig. 2. The differences between the powders are most probably due to the different experimental setups.

The target oven temperature was then calibrated against the applied heating current, with pre-installed thermocouples contrary to the usual use of a pyrometer. The ion-source was calibrated using a pyrometer, following the conventional procedure. The target unit was then mounted at the ISOLDE off-line separator to check for proper operation and beam contaminations. The obtained mass spectrum in the range of interest can be observed on Fig. 3. The <sup>35</sup>Ar beam had to be delivered pure for the physics experiment [17,16] therefore <sup>35</sup>Cl had to be low. From Fig. 3, <sup>35</sup>Cl was around 10 pA, decreasing with time. While online the <sup>35</sup>Cl beam current was below the detection limit (~0.5 pA) and much below the measured <sup>35</sup>Ar ion current.

## 2.3. Online tests

The target was mounted on the ISOLDE frontend – GPS (General Purpose Separator) – in November 2011 and release measurements were assessed for 8 h before the physics program with the requested isotopes: <sup>35</sup>Ar, <sup>32</sup>Ar and <sup>31</sup>Ar.

The release profile of the isotopes after each proton pulse was studied at the ISOLDE tape station [26] and has a pulse shape generally approximated by [27]:

$$P(t) = \frac{1}{\text{Norm}} (1 - e^{-\lambda_r t}) [\alpha e^{-\lambda_f t} + (1 - \alpha) e^{-\lambda_s t}] \quad (3)$$

where  $\lambda_r, \lambda_f, \lambda_s$ , are the time-constant parameters (which can take the form of  $\lambda_x = \ln(2)/t_x$ ) and  $\alpha$  is a weighting factor between  $\lambda_f$  and  $\lambda_s$ . The measurements of all isotopes, except for  $^{31,32}\text{Ar}$ , were made using the tape station where the isotopes of interest are implanted on a mylar tape for a defined time ( $t_c$ ) after a certain delay time from the proton impact ( $t_d$ ), which is then moved to the front of  $\beta$  and  $\gamma$  detectors. The count rates are then corrected for decay time during transport and the results are fitted with Eq. 3. The yield is calculated from the integration of this term over time and normalized to the proton current (in ions  $\mu\text{C}^{-1}$ ).

By injecting a known flux of stable Ar into the ion source, with the use of a calibrated leak and measuring the obtained ion current,  $\varepsilon_{is}$  was determined. Using the stable argon beam ( $^{40}\text{Ar}^+$ ),  $\varepsilon_{trans}$  was extracted by measuring the ion currents along the beam line, up to the tape station position. The release efficiency of the target material ( $\varepsilon_{rel}$ ) can be extracted from the simulation of the in-target production for certain isotopes ( $Y_{prod}$ ), using the simulation code ABRABLA [28,29]:

$$\varepsilon_{rel} = \frac{Y_{obs}}{Y_{prod} \varepsilon_{is}} \quad (4)$$

where  $Y_{obs}$  is the measured yield corrected for  $\varepsilon_{trans}$ .

The yields of  $^{31-33}\text{Ar}$  were measured by an experimental setup described in [18], by measuring  $\beta$ -delayed proton emission (ISOLDE Experiment, IS476 [14]).  $^{33}\text{Ar}$  was also measured using the tape station and the setup described above, in order to compare and determine the beam transport efficiency ( $\varepsilon_{trans}$ ) to the experimental setup. As  $^{33}\text{Cl}$  was a contamination and a decay product, the differentiation between  $^{33}\text{Ar}$  and  $^{33}\text{Cl}$  was done through fitting the overall decay curve with the two half-lives respectively.  $^{34}\text{Ar}$  was measured using the gamma detector of the tape station.

### 3. Results and discussion

In order to have an acceptable  $^{35}\text{Ar}$  beam for the experiment and assure stable operation, the temperatures were set at 690 °C

**Table 4**  
Yield values of the studied isotopes released from the nanostructured calcium oxide target. The respective temperatures of the target oven and ion source as well as in-target production, derived release efficiencies ( $\varepsilon_{rel}$ ) and times of measurement are also included. Database values [13], usually measured after 8 h of operation, are also introduced in parenthesis.

Isotope	$T_{1/2}$	Target temperature center (and side) (°C)	Ion source temperature (°C)	Online operation time (h)	$Y_{obs}$	$(Y_{db})$	$Y_{prod}$ #469 (ABRABLA) ions $\mu\text{C}^{-1}$	$\varepsilon_{rel}$ (%)
					ions $\mu\text{C}^{-1}$			
$^{31}\text{Ar}$	15.1 ms	568 (687)	2020 ± 50	86 (8/32)	34 ± 13 <sup>a</sup>	(5/1)	1.9 × 10 <sup>4</sup>	– (0.2)
$^{32}\text{Ar}$	98 ms	568 (687)	1970	86	2600 <sup>a</sup>	(3300)	6.7 × 10 <sup>5</sup>	4.9 (10.0)
$^{33}\text{Ar}$	174.1 ms	568 (687)	1970	86	1.2 × 10 <sup>5</sup>	(3.8 × 10 <sup>4</sup> )	1.2 × 10 <sup>7</sup>	12.8 (6.6)
$^{34}\text{Ar}$	844 ms	568 (687)	1970	86	1.7 × 10 <sup>6</sup>	(1.7 × 10 <sup>6</sup> ) <sup>b</sup>	1.8 × 10 <sup>8</sup>	12.2 (44.0)
$^{35}\text{Ar}$	1.78 s	389 (576)	1970	12	4.7 × 10 <sup>6</sup>	(4.3 × 10 <sup>7</sup> )	2.0 × 10 <sup>9</sup>	3.3 (43.9)
$^{35}\text{Ar}$	1.78 s	568 (687)	1970	– <sup>c</sup>	3.2 × 10 <sup>7</sup> <sup>c</sup>	(4.3 × 10 <sup>7</sup> )	2.0 × 10 <sup>9</sup>	20.2 (43.9)
$^{35}\text{Ar}$	1.78 s	677 (758)	2070	13	5.3 × 10 <sup>7</sup>	(4.3 × 10 <sup>7</sup> )	2.0 × 10 <sup>9</sup>	43.8 (43.9)
$^{35}\text{Ar}$	1.78 s	817 (857)	2070	88	2.0 × 10 <sup>8</sup> <sup>d</sup>	(4.3 × 10 <sup>7</sup> )	2.0 × 10 <sup>9</sup>	52.0 (43.9)
$^6\text{He}$	806.7 ms	568 (687)	1970	16	2.3 × 10 <sup>6</sup>	(2.6 × 10 <sup>6</sup> ) <sup>e</sup>	–	– <sup>f</sup>
$^{19}\text{Ne}$	17.22 s	568 (687)	1970	9	9.6 × 10 <sup>6</sup>	(7.5 × 10 <sup>6</sup> ) <sup>e</sup>	1.4 × 10 <sup>9</sup>	– <sup>f</sup>
$^{10}\text{C}^{16}\text{O}$	19.3 s	389 (576)	1970	12	1.2 × 10 <sup>5</sup>	(5.3 × 10 <sup>5</sup> )	2.0 × 10 <sup>8</sup>	– <sup>f</sup>
$^{10}\text{C}^{16}\text{O}$	19.3 s	677 (758)	1970	13	7.0 × 10 <sup>5</sup>	(5.3 × 10 <sup>5</sup> )	2.0 × 10 <sup>8</sup>	– <sup>f</sup>
$^{15}\text{C}^{16}\text{O}$	2.45 s	568 (687)	1970	9	7.9 × 10 <sup>4</sup>	(6.2 × 10 <sup>3</sup> )	1.7 × 10 <sup>7</sup>	– <sup>f</sup>
$^{15}\text{C}^{16}\text{O}$	2.45 s	677 (758)	1970	13	1.5 × 10 <sup>5</sup>	(6.2 × 10 <sup>3</sup> )	1.7 × 10 <sup>7</sup>	– <sup>f</sup>

<sup>a</sup> Yield determined by IS476 (scaled for loss factor, see text).

<sup>b</sup> A higher yield (3.8 × 10<sup>6</sup> ions  $\mu\text{C}^{-1}$ ) exists from the Synchro-cyclotron, which supplied a continuous wave proton beam of 600 MeV.

<sup>c</sup> Average yield along the run (see Fig. 4) at nominal target and ion-source temperatures defined for the run.

<sup>d</sup> Underestimated yield due to detector saturation.

<sup>e</sup> Database yields of CaO, higher yields from other target materials exist in these cases:  $^6\text{He}$  – 4.7 × 10<sup>7</sup> ions  $\mu\text{C}^{-1}$  – UC<sub>x</sub> target,  $^{19}\text{Ne}$  – 3.0 × 10<sup>7</sup> ions  $\mu\text{C}^{-1}$  – MgO target.

<sup>f</sup> Element ionization efficiency not determined.

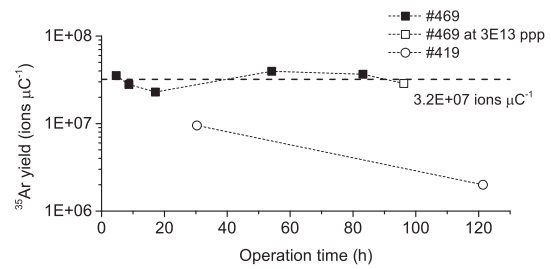


**Fig. 4.**  $^{35}\text{Ar}$  yield variation for two CaO ISOLDE targets during the runs, #469 operated at nominal temperatures (see Table 4) with  $8 \times 10^{12}$  ppp – the one from this work – and #419 operated in November 2009 at  $3 \times 10^{13}$  ppp. The dashed line represents the average yield along the #469 run.

for the target thermocouples and 1970 °C for the ion source (corresponding to ~8% ionization efficiency). The proton intensity of  $8 \times 10^{12}$  protons per pulse (ppp) was chosen to reduce the thermal stresses imposed to the target material by the proton pulse. Temperatures were changed to investigate the detailed release properties. Overall, the yields from the target #469 matched and surpassed database record yields ( $Y_{db}$ ) at ISOLDE (Table 4) [13].

The  $^{35}\text{Ar}$  yield, at nominal target operation temperatures (568 °C – center thermocouple), fluctuated by no more than a factor 2 between  $2.3 \times 10^7$  and  $4.0 \times 10^7$  ions  $\mu\text{C}^{-1}$ , with an average of  $3.2 \times 10^7$  ions  $\mu\text{C}^{-1}$  throughout the run (Fig. 4). This values match the database yield ( $4.3 \times 10^7$  ions  $\mu\text{C}^{-1}$ ) ([13]) – as in Table 4), however the main achievement of this target was its stability throughout the ~100 h of the run, solving the problem from the past (see comparison, in Fig. 4, with another CaO target – #419 – from November 2009, considered one of the best operated at ISOLDE in the past years). The respective time components from Eq. 3 from the release curves taken on  $^{35}\text{Ar}$  were very similar (Fig. 5), indicating no change in the material and unit, i.e. no sintering.

Ravn and his collaborators [12] also studied the release of noble gases in CaO targets. In the referred work  $^{35}\text{Ar}$  yields were measured under two target temperatures: operating temperatures (950 °C) and at much higher ones (1420 °C). The yields of  $^{33-35}\text{Ar}$  at operating temperatures were one order of magnitude (or more)



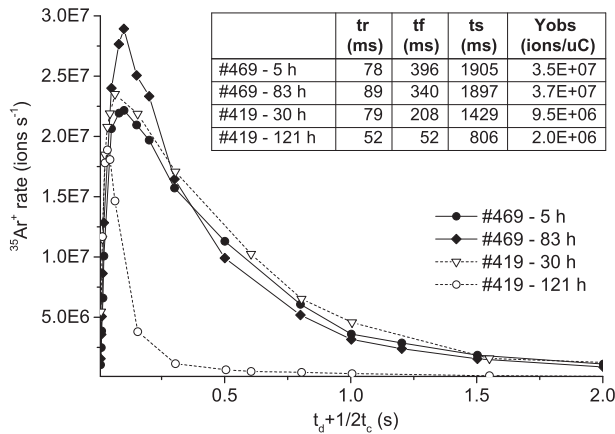


Fig. 5. Release time structure of  $^{35}\text{Ar}$  after one pulse, from target #419 with  $3 \times 10^{13}$  ppp, at the beginning (30 h) and end of the run (121 h). For target #469 the two release curves are presented in the same way ( $8 \times 10^{12}$  ppp). In each case the operation temperatures were kept throughout the run.

lower than in the case of the target produced and operated under the newly defined procedure, which was at a lower operating temperature, while the high temperature settings in both targets produced the same yield of  $^{35}\text{Ar}$  ( $2.0 \times 10^8$  ions  $\mu\text{C}^{-1}$ ). However no information is given on the yield stability, besides a statement that oxide targets are stable at least for the first 48 h [12]. However, the sintering studies performed in this work have proven that this material would sinter considerably, if the high temperature operation settings were kept.

Fig. 5 shows release curves and respective release times for  $^{35}\text{Ar}$  of the target studied in this work compared to an older target – #419 (already referred before in the text and also present in Fig. 4).

The release curves are represented in ions  $\text{s}^{-1}$ , in order to account for the different proton intensities (3.75 times lower intensity in the #469 target). Note that also, different operating temperatures – 687 °C (side thermocouple) compared to 950 °C of the #419, were chosen. Even though, having lower proton intensities and a lower temperature, this target can generate a similar  $^{35}\text{Ar}$  ion pulse intensity to the #419 target. However the time structure of the release curve of the #419 target at the beginning, was lost over time. Instead an apparent faster release but with a much lower yield was obtained, which can be related to the microstructure change.

Due to the known CaO yield degradation in previous units, the measurement of very exotic isotopes yields (like  $^{31,32}\text{Ar}$  with  $T_{1/2}$  of 15.1 and 98 ms, respectively) would usually be assessed at the very beginning of operation and when they would decay to a small fraction of the initial value in a matter of hours (see database values on  $^{31}\text{Ar}$  on Table 4). Due to schedule constraints in the operation of this target, it was only possible to measure the yields after 86 h of operation of the CaO target from this work (#469). The obtained yields of  $^{31}\text{Ar}$ , summarized in Table 4, were very high compared to previous records at ISOLDE (5 which would decay to the usual 1 ion  $\mu\text{C}^{-1}$  after a few hours) [25,13]. However, as referenced in subsection 2.3, the  $^{33}\text{Ar}$  yield was determined at the tape station and at the IS476 experiment with a factor  $\sim 3.8$  lower yield in the later measurement. We interpret this as a loss in beam transmission to the detector of IS476, the reason being investigated. As so, the values of  $^{31,32}\text{Ar}$  presented in Table 4 are corrected with this factor. Nonetheless, the  $^{31}\text{Ar}$  yield value indicates not only that the target material is very stable but also that the nanostructured CaO provides, at lower temperatures, higher yields of exotic noble gas isotopes, probably due to the reduction of the diffusion lengths and SSA increase. The  $^{32}\text{Ar}$  was surprisingly lower than from older

targets, much probably due to a transmission problem and the  $^{34}\text{Ar}$  yield matched previous values. However, both  $^{31}\text{Ar}$  and  $^{33}\text{Ar}$  displayed an increased yield, by a threefold and seven fold, respectively (see Table 4).

When the diffusion times (average time it takes for an element to diffuse out of a grain) are larger than the isotope half-life, the isotopes decay before they can reach the surface of a grain. This will result in less isotopes being released (lower yields) with faster release times, since diffusion processes are generally associated with the long tail of a release curve. This effect is more important the shorter the half-life, as demonstrated experimentally from the calculated  $\varepsilon_{rel}$  of  $^{32-35}\text{Ar}$  (Table 4). The temperature also plays a very important role in the yields and so in  $\varepsilon_{rel}$  (Table 4), since it affects both effusion and diffusion processes (Eq. 2). However if the temperature is too high, it can lead to microstructure degradation as demonstrated by the change to a faster release time and lower yield of the #419 target (Fig. 5). This degradation happens through a sintering process (through high temperature and/or high proton intensity) resulting in larger grain sizes, making release processes through diffusion less and less dominant. The  $\varepsilon_{rel}$  of old CaO targets, are comparable to the ones of this target. However as already discussed before, CaO target yields in the past would decay to a fraction of the initial value, once more showing the importance of the microstructure in the release. The diffusion and effusion processes have been quantitatively related before with the release profile of an isotope [3,30,31], which will also be attempted for this work in a future report.

Apart from the argon yields, other elements (C, Ne and He) were measured as well and are presented on Table 4. The  $^{15}\text{C}^{16}\text{O}$  yield was up to almost 25 times higher than database values,  $^{10}\text{C}^{16}\text{O}$  and  $^{19}\text{Ne}$  isotope yields were slightly higher than CaO target database values while the yield of  $^6\text{He}$  was slightly lower [13].

#### 4. Conclusion

Highly porous nanostructured CaO material with a high specific surface area was successfully produced and used online, making it the first nanostructured target to be operated at ISOLDE-CERN. Improved target production, handling and operation procedures were proposed and applied. The material was irradiated with pulsed energetic protons for isotope beam production and the yields obtained are as high or higher than previous CaO targets. The most important achievement was the stability of the intensity of the produced beams, as shown for  $^{35}\text{Ar}$  and for the very exotic isotopes ( $^{31-33}\text{Ar}$ ).

In ISOL facilities the paradigm of setting the operation temperature as high as possible is very common, harming most of the times the long term yield performance of a target, by microstructure degradation. As shown in this study the highest temperature is not the most important factor for a high yield, especially if one expects it to be stable. A fine structure (sub-micron or nano) with high porosity, as reported here, has shown a big advantage: even though the operation temperature had to be lowered to keep such structure, the obtained yields were as high as previous targets and even higher in the case of the short lived isotopes. In addition they were stable during operation, which had not been observed in the past. In the future this concept can, in principle, be applied to other target materials, enlarging the family of submicron and nanostructured materials already developed for ISOL facilities.

#### Acknowledgements

The author J.P. Ramos gratefully acknowledges Bernard Crepioux, Michael Owen and Ermanno Barbero for the technical support and the financial support from Agência de Inovação, S.A. (AdI) and

CERN, through the Grant SFRH/ BEST/ 51352/ 2011 for the traineeship at CERN.

## References

- [1] E. Kugler, *The ISOLDE facility*, *Hyperfine Interact.* 129 (2000) 23–42.
- [2] U. Köster, Intense radioactive-ion beams produced with the ISOL method, *Eur. Phys. J. A – Hadrons Nuclei* 15 (2002) 255–263, <http://dx.doi.org/10.1140/epja/i2001-10264-2>.
- [3] R. Kirchner, On the release and ionization efficiency of catcher-ion-source systems in isotope separation on-line, *Nucl. Instrum. Methods Phys. Res. Sect. B: Beam Interact. Mater. Atoms* 70 (1992) 186–199.
- [4] S. Fernandes, R. Bruetsch, R. Catherall, F. Groeschel, I. Guenther-Leopold, J. Lettry, E. Manfrin, S. Marzari, E. Noah, S. Sgobba, T. Stora, L. Zanini, Microstructure evolution of nanostructured and submicrometric porous refractory ceramics induced by a continuous high-energy proton beam, *J. Nucl. Mater.* 416 (2011) 99–110. *Nuclear Materials* IV.
- [5] R. Kirchner, Release studies of elementary and metal-fluoride ions at the GSI on-line mass separator, *Nucl. Instrum. Methods Phys. Res. Sect. B: Beam Interact. Mater. Atoms* 126 (1997) 135–140.
- [6] S.-J.L. Kang, *Sintering: Densification, Grain Growth, and Microstructure*, Elsevier, Oxford, 2005.
- [7] T. Stora, E. Bouquerel, L. Bruno, R. Catherall, S. Fernandes, P. Kasprovicz, J. Lettry, S. Marzari, B.S.N. Singh, E. Noah, L. Penescu, R. Wilfinger, Oxide target designs for high primary beam intensities for future radioactive ion beam facilities, *AIP Conf. Proc.* 1099 (2009) 764–768.
- [8] L. Penescu, Techniques to produce and accelerate radioactive ion beams (PhD thesis) University “Politehnica” Bucharest, 2009.
- [9] S. Fernandes, Submicro- and nano-structured porous materials for production of high-intensity exotic radioactive ion beams (PhD thesis), Ecole Polytechnique Fédérale de Lausanne EPFL, Lausanne, 2010. CERN-THESIS-2010-170.
- [10] M. Dombbsky, L. Buchmann, J.M. D’Auria, P. McNeely, G. Roy, H. Sprenger, J. Vincent, Targets and ion sources at the TISOL facility, *Nucl. Instrum. Methods Phys. Res. Sect. B: Beam Interact. Mater. Atoms* 70 (1992) 125–130.
- [11] T. Björnstad, M.J.G. Borge, P. Dessagne, R.D. Von Dincklage, G.T. Ewan, P.G. Hansen, A. Huck, B. Jonson, G. Klotz, A. Knipper, P.O. Larsson, G. Nyman, H.L. Ravn, C. Richard-Serre, K. Riisager, D. Schardt, G. Walter, Study of the giant gamow-teller resonance in nuclear  $\beta$ -decay: the case of  $^{32}\text{Ar}$ , *Nucl. Phys. A* 443 (1985) 283–301.
- [12] H.L. Ravn, R. Catherall, J. Barker, P. Drumm, A.H.M. Evensen, E. Hageb, P. Hoff, O.C. Jonsson, E. Kugler, J. Lettry, K. Steffensen, O. Tengblad, the ISOLDE Collaboration, Bunched release of gases from oxide targets, *Nucl. Instrum. Methods Phys. Res. Sect. B: Beam Interact. Mater. Atoms* 126 (1997) 176–181 (International Conference on Electromagnetic Isotope Separators and Techniques Related to their Applications).
- [13] M. Turrion, H.-I. Urszula, ISOLDE yield database. <<https://oraweb.cern.ch/pls/isolde/querytgt>>, 2012
- [14] H.O.U. Fynbo, L. Audirac, B. Blank, B.J.G. Borge, G. Ganchel, M. Carmona-Gallardo, R. Dominguez-Reyes, L.M. Fraile, D. Galaviz, J. Giovinazzo, S. Hyldegaard, H.B. Jeppesen, J.S. Johansen, A. Jokinen, B. Jonson, O.S. Kirsebom, T. Kurtukian-Nieto, I. Matea, T. Nilsson, G. Nyman, K. Riisager, J. Souin, O. Tengblad, E. Tengborn, J.C. Thomas, J. Åystö, Studies of  $\beta$ -delayed two-proton emission: the cases of  $^{31}\text{Ar}$  and  $^{39}\text{Ca}$ , 2008, CERN INTC Proposal, INTC-P-248.
- [15] S. Kreim, D. Beck, K. Blaum, C. Böhm, C. Borgmann, M. Breitenfeldt, T. Eronen, F. Herfurth, M. Kowalska, D. Lunney, V. Manea, S. Naimi, D. Neidherr, M. Rosenbusch, L. Schweikhard, J. Stanja, F. Wienholtz, R.N. Wolf, K. Zuber, A. Kankainen, J. Collaboration, Remeasurement of  $^{32}\text{Ar}$  to test IMME, 2012, CERN INTC Proposal, INTC-P-332.
- [16] D. Beck, M. Beck, T. Phalet, P. Schuurmans, N. Severijns, A. Van Geert, B. Vereecke, S. Versyck, J. Deutsch, R. Prieels, G. Bollen, O. Forstner, J. Dilling, W. Quint, F. Ames, P. Schmidt, Proposal to the ISOLDE Scientific Committee: search for new physics in beta-neutrino correlations using trapped ions and a retardation spectrometer, 1999, CERN ISC Proposal, ISC/P111.
- [17] S. Van Gorp, et al. First recoil energy spectrum from  $\beta$  decay of ions stored in a Penning trap, (submitted for publication); M. Breitenfeldt for IS433, ISOLDE Newsletter, p. 8, 2013. URL <<http://isolde.web.cern.ch/sites/isolde.web.cern.ch/files/April2013.pdf>>.
- [18] H.O.U. Fynbo, M.J.G. Borge, L. Axelsson, J. Åystö, U.C. Bergmann, L.M. Fraile, A. Honkanen, P. Hornshj, Y. Jading, A. Jokinen, B. Jonson, I. Martel, I. Mukha, T. Nilsson, G. Nyman, M. Oinonen, I. Piqueras, K. Riisager, T. Siiskonen, M.H. Smedberg, O. Tengblad, J. Thaysen, F. Wenander, and the ISOLDE Collaboration, The  $\beta 2p$  decay mechanism of  $^{31}\text{Ar}$ , *Nucl. Phys. A* 677 (2000) 38–60.
- [19] G.T. Koldste, B. Blank, M.J.G. Borge, J.A. Briz, M. Carmona-Gallardo, L.M. Fraile, H.O.U. Fynbo, J. Giovinazzo, J.G. Johansen, A. Jokinen, B. Jonson, T. Kurtukian-Nieto, J.H. Kusk, T. Nilsson, A. Perea, V. Pseudo, E. Picado, K. Riisager, A. Saastamoinen, O. Tengblad, J.-C. Thomas, J. Van de Walle, Relative proton and  $\gamma$  widths of astrophysically important states in  $^{30}\text{S}$  studied in the  $\beta$ -delayed decay of  $^{31}\text{Ar}$ , *Phys. Rev. C* 87 (2013) 055808.
- [20] J.P. Ramos, C.M. Fernandes, A.M.R. Senos, T. Stora, Sintering kinetics of nanometric calcium oxide in vacuum atmosphere, 2013 (in preparation).
- [21] J.P. Ramos, Effect of Calcium Oxide Microstructure on the Diffusion of Isotopes (Master’s thesis), University of Aveiro, Aveiro, 2012, CERN-THESIS-2012-008.
- [22] S. Brunauer, P.H. Emmett, E. Teller, Adsorption of gases in multimolecular layers, *J. Am. Chem. Soc.* 60 (1938) 309–319.
- [23] E.P. Barrett, L.G. Joyner, P.P. Halenda, The determination of pore volume and area distributions in porous substances. I. Computations from nitrogen isotherms, *J. Am. Chem. Soc.* 73 (1951) 373–380.
- [24] J.I. Langford, A.J.C. Wilson, Scherrer after sixty years: a survey and some new results in the determination of crystallite size, *J. Appl. Crystallogr.* 11 (1978) 102–113.
- [25] L. Penescu, R. Catherall, J. Lettry, T. Stora, Development of high efficiency Versatile Arc Discharge Ion Source at CERN ISOLDE, *Rev. Sci. Instrum.* 81 (2010) 02A906.
- [26] M. Turrión, M. Eller, R. Catherall, L.M. Fraile, U. Herman-Izycka, U. Köster, J. Lettry, K. Riisager, T. Stora, Management of ISOLDE yields, *Nucl. Instrum. Methods Phys. Res. Sect. B: Beam Interact. Mater. Atoms* 266 (2008) 4674–4677.
- [27] J. Lettry, R. Catherall, P. Drumm, P. Van Duppen, A.H.M. Evensen, G.J. Focker, A. Jokinen, O.C. Jonsson, E. Kugler, H. Ravn, Pulse shape of the ISOLDE radioactive ion beams, *Nucl. Instrum. Methods Phys. Res. Sect. B: Beam Interact. Mater. Atoms* 126 (1997) 130–134.
- [28] A.R. Junghans, M. de Jong, H.-G. Clerc, A.V. Ignatyuk, G.A. Kudyaev, K.-H. Schmidt, Projectile-fragment yields as a probe for the collective enhancement in the nuclear level density, *Nucl. Phys. A* 629 (1998) 635–655.
- [29] J.-J. Gaimard, K.-H. Schmidt, A reexamination of the abrasion-ablation model for the description of the nuclear fragmentation reaction, *Nucl. Phys. A* 531 (1991) 709–745.
- [30] E. Bouquerel, J. Lettry, T. Stora, Atomic beam merging and suppression of alkali contaminants in multi body high power targets: design and test of target and ion source prototypes at ISOLDE (PhD thesis), Université Paris XI, 2009.
- [31] T. Stora, E. Noah, R. Hodak, T.Y. Hirsh, M. Hass, V. Kumar, K. Singh, S. Vaintraub, P. Delahaye, H. Franberg-Delahaye, M.-G. Saint-Laurent, G. Lheronneau, A high intensity  $^6\text{He}$  beam for the  $\beta$ -beam neutrino oscillation facility, *EPL (Europhys. Lett.)* 98 (2012) 32001.